Konuralp Journal of Mathematics, 10 (2) (2022) 220-232

Konuralp Journal of Mathematics

Research Paper

Journal Homepage: www.dergipark.gov.tr/konuralpjournalmath

e-ISSN: 2147-625X

Two Effective Numerical Approaches for Equal Width Wave (EW) Equation Using Lie- Trotter Splitting Technique

Melike Karta[1]

[1]*Department of Mathematics, Faculty of Science and Arts, Ağrı İbrahim Çeçen University,Ağrı,Turkey*

Abstract

In this work, approximate solutions of the EW equation are obtained by two influential numerical schemes. For the first and second method, after splitting equal width wave (EW) equation in time, it is solved by Lie- Trotter splitting technique via quintic B-spline Collocation and cubic B-spline Lumped Galerkin FEMs and the suited finite difference approaches for space and time discretizations respectively. Stability analysis of schemes is made and both schemes are implemented and tested by two example The acquired numerical results are compared with those in the literature with the help of the error norms and conservation features. It is seen that the error norms are quite small, the present conservation constants are consistent according to the results compared.

Keywords: *B-splines; Collocation method; Lumped Galerkin method; Equal Width Equation; Lie- Trotter splitting.*

2010 Mathematics Subject Classification: *2000 MSC: 35Q51; 74J35; 33F10.*

1. Introduction

The EW equation, which is a one-dimensional PDE as an equally valid and accurate model for the same wave phenomena simulated by the KdV and RLW equations [9] is presented in the following form , was proposed by Morrison *et al.* [1]

$$U_t - \varepsilon U_{xxt} + UU_x = 0, \tag{1.1}$$

where ε is a positive constant and x and t indicate spatial and temporal variables subindexes. Many different techniques have been proposed for approximate solutions of the equation until today. Among them, we can give as examples studies like collocation method used by Dağ and Saka [2], Raslan [3], Irk *et al.* [4], Fazal-i *et al.* [5], Galerkin method proposed by Dogan [6], Gardner and Gardner [7], Güleç [8], and also the method of lines (MOL) sought by Banaja and Bakodah [9], space-splitting technique and Galerkin method applied by Saka [10], A linearized implicit finite difference method examined by Esen and Kutluay [11], lumped Galerkin method utilized by Esen [12], a least-squares technique implemented by Zaki[13], A Petrov-Galerkin Method investigated by (Roshan[15], Gardner *et al.* [16]), Splitting method by cubic -B splines used by İhsan [17], Trigonometric Cubic B-spline Collocation Method suggested by Yağmurlu and Karakaş [18]. In this study, we are going to seek the approximate solutions of the EW equation with the initial and the boundary conditions

$$U(x,0) = f(x), \qquad x_L \le x \le x_R \tag{1.2}$$

$$\begin{aligned} &U(x_L,t) = U(x_R,t) = 0, \\ &U_x(x_L,t) = U_x(x_R,t) = 0, \quad t > 0 \end{aligned} \tag{1.3}$$

using Lie- Trotter splitting technique via quintic B-spline Collocation and cubic B-spline lumped Galerkin FEMs. To tell the truth, both methods have been used extensively in applications of different partial differential equations. As a result, when the literature is examined, it can be said that there are very good results for the approximate solutions of PDEs. Our aim throughout the study will be to achieve better results with Lie- Trotter splitting technique for both methods.

***Email addresses*: mkarta@agri.edu.tr (M.Karta)**

2. Quintic and Cubic B-Splines

The position $[x_L, x_R]$ and time $[0,T]$ regions are uniformly divided respectively such that $x_L = x_0 < x_1 < ... < x_N = x_R$ and $0 = t_0 < t_1 < ... < t_M = T$. These uniform partitions for the position and the time domains are expressed as $h = x_{j+1} - x_j$ for $j = 0(1)N-1$, and $k = t_{n+1} - t_n$ for $n = 0(1)M-1$, respectively. The quintic B-spline shape functions $\varphi_j(x)$ for $j = -2(1)N+2$ are given as [29]

$$\varphi_j(x) = \frac{1}{h^5}\begin{cases} p_0 = (x-x_{j-3})^5, & x \in [x_{j-3}, x_{j-2}] \\ p_1 = p_0 - 6(x-x_{j-2})^5, & x \in [x_{j-2}, x_{j-1}] \\ p_2 = p_1 - 6(x-x_{j-2})^5 + 15(x-x_{j-1})^5, & x \in [x_{j-1}, x_j] \\ p_3 = p_2 - 6(x-x_{j-2})^5 - 20(x-x_j)^5, & x \in [x_j, x_{j+1}] \\ p_4 = p_3 - 6(x-x_{j-2})^5 + 15(x-x_{j+1})^5, & x \in [x_{j+1}, x_{j+2}] \\ p_5 = p_4 - 6(x-x_{j-2})^5 - 6(x-x_{j+2})^5, & x \in [x_{j+2}, x_{j+3}] \\ 0, & \text{otherwise.} \end{cases} \tag{2.1}$$

and the cubic B-spline shape functions $\phi_j(x)$ for $j = -1(1)N+1$ are given as [29]

$$\varphi_j(x) = \frac{1}{h^3}\begin{cases} r_0 = (x-x_{j-2})^3, & x \in [x_{j-2}, x_{j-1}) \\ r_1 = h^3 + 3h^2(x-x_{j-1}) + 3h(x-x_{j-1})^2 - 3(x-x_{j-1})^3, & x \in [x_{j-1}, x_j) \\ r_2 = h^3 + 3h^2(x_{j+1}-x) + 3h(x_{j+1}-x)^2 - 3(x_{j+1}-x)^3, & x \in [x_j, x_{j+1}) \\ r_3 = (x_{j+2}-x)^3, & x \in [x_{j+1}, x_{j+2}] \\ 0, & \text{otherwise.} \end{cases} \tag{2.2}$$

The whole of quintic B-spline base functions $\varphi_{-2}(x), \varphi_{-1}(x), \ldots, \varphi_{N+2}(x)$ forming a base for the functions defined on $[x_L, x_R]$ are zero outside of $\phi_{j-2}, \varphi_{j-1}, \varphi_j, \varphi_{j+1}, \varphi_{j+2}$, and φ_{j+3}. Furhermore, the whole of cubic B-spline bases functions $\varphi_{-1}(x), ..., \varphi_{N+1}(x)$ are zero outside of $\varphi_{j-1}, \varphi_j, \varphi_{j+1}, \varphi_{j+2}$. Therefore, on a typical element $[x_j, x_{j+1}]$ via the local coordinate transformation described as $h = x - x_j$, $0 \le \zeta \le h$, the quintic and cubic B-spline bases functions on $[0,h]$ for variable ζ are expressed in form

$$\begin{aligned} \varphi_{j-2} &= 1 - 5\zeta + 10\zeta^2 - 10\zeta^3 + 5\zeta^4 - \zeta^5, \\ \varphi_{j-1} &= 26 - 50\zeta + 20\zeta^2 + 20\zeta^3 - 20\zeta^4 + 5\zeta^5, \\ \varphi_j &= 66 - 60\zeta^2 + 30\zeta^4 - 10\zeta^5, \\ \varphi_{j+1} &= 26 + 50\zeta + 20\zeta^2 - 20\zeta^3 - 20\zeta^4 + 10\zeta^5, \\ \varphi_{j+2} &= 1 + 5\zeta + 10\zeta^2 + 10\zeta^3 + 5\zeta^4 - 5\zeta^5, \\ \varphi_{j+3} &= \zeta^5. \end{aligned} \tag{2.3}$$

and

$$\begin{aligned} \varphi_{j-1} &= (1-\zeta)^3, \\ \varphi_j &= 1 + 3(1-\zeta) + 3(1-\zeta)^2 - 3(1-\zeta)^3, \\ \varphi_{j+1} &= 1 + 3\zeta + 3\xi^2 - 3\zeta^3, \\ \varphi_{j+2} &= \zeta^3. \end{aligned} \tag{2.4}$$

3. Scheme I: Lie-trotter Splitting Collocation FEM with Qintic B-Spline

The numerical results of EW equation are going to be found by Lie- Trotter splitting technique [30] combined with quintic B-spline collocation method. For this cause, EW equation is split into two sub-equations in the following form providing linear and nonlinear respectively ,

$$U_t - \varepsilon U_{xxt} = 0 \tag{3.1}$$

$$U_t - \varepsilon U_{xxt} + UU_x = 0. \tag{3.2}$$

Each of them is solved on its time interval $[t_n, t_{n+1}]$. To prevent any mess, we utilize u and y instead of U in Eqs. (3.1) and (3.2). So, the Lie-Trotter splitting algorithm of equations is obtained in the following form

$$u_t - \varepsilon u_{xxt} = 0$$

$$u(x,t_n) = U(x,t_n), \quad t \in [t_n, t_{n+1}], \tag{3.3}$$

$$y_t - \varepsilon y_{xxt} + yy_x = 0$$

$$y(x,t_n) = u(x,t_{n+1}), \quad t \in [t_n, t_{n+1}], \tag{3.4}$$

in which $t_{n+1}=(n+1)k$. For convenience, let the discretized forms of the derivatives of the dependent variables u and y in Eqs.(3.3) and (3.4) be submitted as

$$(.)_t=\frac{(.)^{**}-(.)^{*}}{\Delta t},\quad (.)_{xxt}=\frac{(.)^{**}_{xx}-(.)^{*}_{xx}}{\Delta t}, \tag{3.5}$$

$$(.)_x=\frac{(.)^{**}_{x}+(.)^{*}_{x}}{2},\quad (.)_{xx}=\frac{(.)^{**}_{xx}+(.)^{*}_{xx}}{2}. \tag{3.6}$$

If Eqs. (3.5),(3.6) are replaced in (3.3),(3.4), for the time levels n and $n+1$, the following numerical approximations are obtained

$$u^{n+1}-\varepsilon u^{n}_{xx}=u^{n}-\varepsilon u^{n}_{xx}, \tag{3.7}$$

$$y^{n+1}-\varepsilon y^{n+1}_{xx}+\Delta t\frac{Z}{2}y^{n+1}_{x}=y^{n}-\varepsilon y^{n}_{xx}+\Delta t\frac{Z}{2}y^{n}_{x}, \tag{3.8}$$

in which $Z=y$. When we have taken the approximate ones $u_N(x,t),y_N(x,t)$ corresponding to the exact solutions $u(x,t),y(x,t)$ in Eqs.(3.3),(3.4), numerical values $u_N(x_m,t_n),y_N(x_m,t_n)$ at the knot point (x_m,t_n) are shown by u^n_m,y^n_m respectively. The $u_N(x,t),y_N(x,t)$ will be searched in terms of quintic B-spline shape functions $\phi_j(x)$ in form

$$U_N(x,t)=\sum_{j=-2}^{N+2}\varphi_j(x)\delta_j(t),\quad y_N(x,t)=\sum_{j=-2}^{N+2}\varphi_j(x)\Psi_j(t), \tag{3.9}$$

in which $\delta_j(t),\Psi_j(t)$ are unknown time-dependent parameters. Both quintic B-spline functions and their derivatives are zero outside of the domain $[x_{m-3},x_{m+3}]$. For this reason, the numerical results for a typical element$[x_m,x_{m+1}]$ can be given as

$$U_N(x,t)=\sum_{j=m-2}^{m+3}\varphi_j(x)\delta_j(t),\quad y_N(x,t)=\sum_{j=m-2}^{m+3}\varphi_j(x)\Psi_j(t). \tag{3.10}$$

At the point $(x_j,t)(j=0(1)N)$ for any time level, Both the knot values and derivatives of the u_N and y_N can be expressed as

$$\begin{aligned}(.)_j&=()_{j-2}+26()_{j-1}+66()_j+26()_{j+1}+()_{j+2}\\ (.)'_j&=\frac{5}{h}(-()_{j-2}-10()_{j-1}+10()_{j+1}+()_{j+2})\\ (.)''_j&=\frac{20}{h^2}((()_{j-2}+2()_{j-1}-6()_j+2()_{j+1}+()_{j+2}),\end{aligned} \tag{3.11}$$

where unknown time-parameters $\delta_j(t),\Psi_j(t)$ are going to used instead of $()$ in the right hand side of the equalities in Eq.(3.11). If knot values in the (3.11) equalities are substituted in the Eqs.(3.3),(3.4), the following system of algebraic equations are obtained

$$\begin{aligned}&k_1\delta^{n+1}_{m-2}+_2\delta^{n+1}_{m-1}+k_3\delta^{n+1}_{m}+k_4\delta^{n+1}_{m+1}+k_5\delta^{n+1}_{m+2}=\\ &\quad k_5\delta^{n}_{m-2}+k_4\delta^{n}_{m-1}+k_3\delta^{n}_{m}+k_2\delta^{n}_{m+1}+k_1\delta^{n}_{m+2}\end{aligned} \tag{3.12}$$

$$\begin{aligned}&l_1\Psi^{n+1}_{m-2}+l_2\Psi^{n+1}_{m-1}+l_3\Psi^{n+1}_{m}+l_4\Psi^{n+1}_{m+1}+l_5\Psi^{n+1}_{m+2}=\\ &\quad l_6\Psi^{n}_{m-2}+l_7\Psi^{n}_{m-1}+l_8\Psi^{n}_{m}+l_9\Psi^{n}_{m+1}+l_{10}\Psi^{n}_{m+2}\end{aligned} \tag{3.13}$$

in which $k_i,l_i(i=1(1)5),(m=0(1)N)$ and

$$k_1=1-\frac{20\varepsilon}{h^2},k_2=26-\frac{40\varepsilon}{h^2},k_3=66+\frac{120\varepsilon}{h^2},k_4=26-\frac{40\varepsilon}{h^2},k_5=1-\frac{20\varepsilon}{h^2},$$

$$l_1=1-\frac{20\varepsilon}{h^2}-\frac{5\kappa\Delta t}{2h},l_2=26-\frac{40\varepsilon}{h^2}-\frac{25\kappa\Delta t}{h},l_3=66+\frac{120\varepsilon}{h^2},l_4=26-\frac{40\varepsilon}{h^2}+\frac{25\kappa\Delta t}{h},$$

$$l_5=1-\frac{20\varepsilon}{h^2}+\frac{5\kappa\Delta t}{2h},l_6=1-\frac{20\varepsilon}{h^2}+\frac{5\kappa\Delta t}{2h},l_7=26-\frac{40\varepsilon}{h^2}+\frac{25\kappa\Delta t}{h},l_8=66+\frac{120\varepsilon}{h^2},$$

$$l_9=26-\frac{40\varepsilon}{h^2}-\frac{25\kappa\Delta t}{h},l_{10}=1-\frac{20\varepsilon}{h^2}-\frac{5\kappa\Delta t}{2h},$$

where $\kappa=Z_m=y_m$. Above equation systems with the generalized rows (3.12) and (3.13) comprise from (N+5) unknown and (N+1) equations. The unknowns $()_{-1},()_{-2},()_{N+2},()_{N+1}(m=0(1)N-1)$ eliminated from the system utilizing the boundary conditions $(.)(x_L,t)=(.)(x_R,t)=0,(.)_x(x_L,t)=(.)_x(x_R,t)=0$. Therefore, unknown time-parameters $\delta^T=(\delta_0\delta_1...\delta_N)^T$, and $\Psi^T=(\Psi_0\Psi_1...\Psi_N)^T$ are obtained and the two algebraic systems having $N+1$ unknown and $N+1$ equations are emerged. Firstly of all, parameter δ^0 must be known to begin

the iteration process. Then, this parameter is computed from the system of algebraic equations presented in the following form, found from the initial condition and its derivatives in Eq.(1.2)

$$\begin{aligned}
\delta^0_{m-2}+26\delta^0_{m-1}+66\delta^0_m+26\delta^0_{m+1}+\delta^0_{m+2} &= h_0(x_m), m=0(1)N\\
\delta^0_{-2}-10\delta^0_{-1}+10\delta^0_1+\delta^0_2 &= h_0^{'}(x_L)\\
\delta^0_{-2}+2\delta^0_{-1}-6\delta^0_0+2\delta^0_1+\delta^0_2 &= h_0^{''}(x_L)\\
\delta^0_{N-2}+2\delta^0_{N-1}-6\delta^0_N+2\delta^0_{N+1}+\delta^0_{N+2} &= h_0^{''}(x_R)\\
-\delta^0_{N-2}-10\delta^0_{N-1}+10\delta^0_{N+1}+\delta^0_{N+2} &= h_0^{'}(x_R).
\end{aligned} \tag{3.14}$$

Firstly, system (3.12) is computed for δ^{n+1}. Later, the founded values are utilized instead of Ψ^n in system (3.13). The δ^1 parameter is computed via the δ^0 parameter obtained using Eqs.(3.14). The calculation process can be sustained till the requested time level. Furthermore, in order to make better the nonlinear terms in the system (3.13) is implemented an inner iteration presented in form $(\Psi^*)^n=\Psi^n+\frac{1}{2}(\Psi^n-\Psi^{n-1})$ as 3-5 times at each time level.

3.1. Stability Analysis

To obtain the stability analysis of (3.12) and (3.13) systems with the quintic B-spline collocation finite element method, the Fourier method [32] is used. For stability analysis in the nonlinear term yy_x in Equation (3.4), the local constant Z will be used instead of y.Then, $\kappa=Z_m$ in system (3.13) be going to be a constant number. If Fourier modes $\delta^n_j=\rho^n_1 e^{ij\Phi}, \Psi^n_j=\rho^n_2 e^{ij\Phi}$ is replaced in (3.12) and (3.13) systems, respectively and utilized the Euler formula $e^{i\Phi}=cos\Phi+isin\Phi$, it is obtained growth factors presented in the following form

$$\rho_1=\frac{A_1-iB_1}{A_1+iB_1}, \quad \rho_2=\frac{A_1-iC_1}{A_1+iC_1}, \tag{3.15}$$

where

$$A_1=2b_1-\frac{40\varepsilon}{h^2}b_2, B_1=0, C_1=\frac{5\kappa\Delta t}{h}b_3$$

$$b_1=cos2\Phi+26cos\Phi+33, b_2=cos2\Phi+2cos\Phi-3,$$

$$b_3=sin2\Phi+sin\Phi$$

$|\rho_1|=|\rho_2|=1$ from Equation (3.15)) and therefore $|\rho_1|.|\rho_2|=1$. It can be clearly stated that systems (3.12) and (3.13) are unconditionally stable. Because, the conditions $|\rho_1|\leq 1$, and $|\rho_2|\leq 1$ are satisfied.

4. Scheme II: Lie- Trotter Splitting Lumped Galerkin FEM with Cubic B-Spline

In this section, the numerical solutions of EW equation are found by applying Lie- Trotter splitting technique based on cubic B-spline Galerkin FEM, after dividing into as in Eqs. (3.1) and (3.2). We can get the Lie- Trotter splitting algorithm as in (3.3), (3.4) given in section 3. For the problems given by Eqs. (3.3), (3.4), the boundary conditions $U(x_L,t)=U(x_R,t)=0, U_x(x_L,t)=U_x(x_R,t)=0$ are utilized. Eqs. (3.3), (3.4) are integrated on region $[x_L,x_R]$ multiplying by the weight function W. Then, $Z=y$ is taken and applied the partial integration for acquiring weak forms. Let's get the numerical ones $u_N(x,t)$ and $y_N(x,t)$ corresponding to the exact solutions $u(x,t)$ and $y(x,t)$ of Eqs.(3.3) and (3.4), respectively. These approximations can be taken as in (3.9) equality, in terms of cubic B-spline shape functions $\varphi_j(x)$ like in section 2. The approximate solutions over $[0,h]$ with the help of local transformation can be written as follows in terms of σ

$$U_N(\sigma,t)=\sum_{j=m-1}^{m+2}\varphi_j(\sigma)\delta^e_j(t), \quad y_N(\sigma,t)=\sum_{j=m-1}^{m+2}\varphi_j(\sigma)\Psi^e_j. \tag{4.1}$$

Imlementing the local coordinate transformation, the following equations on a typical element e are obtained

$$\int_0^h\left[Wu_t+\varepsilon W_\sigma u_{\sigma t}\right]d\sigma=\varepsilon W u_{\sigma t}\,|_0^h, \tag{4.2}$$

$$\int_0^h\left[Wy_t+\varepsilon W_\sigma y_{\sigma t}+WZ_m y_\sigma\right]d\sigma=\varepsilon W y_{\sigma t}\,|_0^h, \tag{4.3}$$

in which $\kappa=Z_m=y_m$. Here, writing approximation functions u_N, y_N in Eq. (3.9) in place of u, y in Eqs.(4.2) and (4.3) and cubic B-spline functions in place of W, we can acquire

$$\sum_{j=m-1}^{m+2}\left[\left(\int_0^h\varphi_i\varphi_j+\varepsilon\varphi_i^{'}\varphi_j^{'}\right)d\sigma-\varepsilon\varphi_i\varphi_j^{'}\,|_0^h\right]\dot{\delta}_j=0, \tag{4.4}$$

$$\sum_{j=m-1}^{m+2}\left[\left(\int_0^h\varphi_i\varphi_j+\varepsilon\varphi_i^{'}\varphi_j^{'}\right)d\sigma-\varepsilon\varphi_i\varphi_j^{'}\,|_0^h\right]\dot{\Psi}_j+\sum_{j=m-1}^{m+2}\left[\left(\int_0^h Z_m\varphi_i\varphi_j^{'}\right]\Psi_j=0, \tag{4.5}$$

The element matrices A^e, B^e, C^e, E^e on e are computed $(i, j = m-1, m, m+1, m+2)$

$$A^e = \int_0^h \varphi_i \varphi_j d\sigma, B^e = \int_0^h \varphi_i^{'} \varphi_j^{'} d\sigma, C^e = \int_0^h \varphi_i \varphi_j^{'} d\sigma, , E^e = \varphi_i \varphi_j^{'} |_h^0 .$$

If $\delta^e = (\delta^e_{m-1}, \delta^e_m, \delta^e_{m+1}, \delta^e_{m+2})^T$, $\Psi^e = (\Psi^e_{m-1}, \Psi^e_m, \Psi^e_{m+1}, \Psi^e_{m+2})^T$ are gotten, the following equations can be written

$$(A^e + \varepsilon B^e - \varepsilon E^e)\dot{\delta}^e = 0, \tag{4.6}$$

$$(A^e + \varepsilon B^e - \varepsilon E^e)\dot{\Psi}^e + (C_1^e)\Psi^e = 0, \tag{4.7}$$

Here C_1^e is $Z_m C^e$ matrix. As a result of using equations (4.6) and (4.7) on e, global equations are obtained in the following form

$$(A + \varepsilon B - \varepsilon E)\dot{\delta} = 0, \tag{4.8}$$

$$(A + \varepsilon B - \varepsilon E)\dot{\Psi} + (C_1)\Psi = 0. \tag{4.9}$$

The unknowns in the Eqs.(4.8) and (4.9) are $\delta = (\delta_{-1}, \delta_0, ..., \delta_N, \delta_{N+1})^T$, $\Psi = (\Psi_{-1}, \Psi_0, ..., \Psi_N, \Psi_{N+1})^T$, with $N+3$ dimensional and also A, B, C, E are $N+3$ dimensional square matrices and these have generalized rows as follows:

$$A = \frac{1}{140}(1, 120, 1191, 2416, 1191, 120, 1),$$

$$B = \frac{1}{10h}(-3, -72, -45, 240, -45, -72, -3),$$

$$E = (0, 0, 0, 0, 0, 0, 0),$$

$$C = \frac{1}{20}(-1, -56, -245, 0, 245, 56, 1),$$

$$Z_m C = \frac{1}{20}(Z_1, -18Z_1 - 38Z_2, 9Z_1 - 183Z_2 - 71Z_3, 10Z_1 + 150Z_2 - 150Z_3 - 10Z_4, 71Z_2 + 183Z_3 - 9Z_4, 38Z_3 + 18Z_4, Z_4)$$

where $Z_m = \dfrac{U_m + U_{m+1}}{2}$. Substituting discretized forms (3.5),(3.6) given in section 3 in Eqs.(4.8) and (4.9), the following matrix systems are happened

$$(A + \varepsilon B - \varepsilon E)\delta^{n+1} = (A + \varepsilon B - \varepsilon E)\delta^n, \tag{4.10}$$

$$(A + \varepsilon B - \varepsilon E + (C_1)\Delta t/2)\Psi^{n+1} = (A + \varepsilon B - \varepsilon E - (C_1)\Delta t/2)\Psi^n. \tag{4.11}$$

Utilizing the boundary conditions $U(x_L, t) = U(x_R, t) = 0$, the parameters $(\delta_{-3}, \delta_{-2}, \delta_{-1}, \delta_{N+1}, \delta_{N+2}, \delta_{N+3})$, $(\Psi_{-3}, \Psi_{-2}, \Psi_{-1}, \Psi_{N+1}, \Psi_{N+2}, \Psi_{N+3})$ from systems (4.10),(4.11) are removed and $\delta = (\delta_0, \delta_1, ..., \delta_N)^T$, $\Psi = (\Psi_0, \Psi_1, ..., \Psi_N)^T$ are unknown parameters and each of them are $N+1$ dimensional. Thus, $(N+1)x(N+1)$ matrix system is obtained. In order to make better the nonlinear terms in the system (4.11) is implemented an inner iteration submitted as in section 1. At the point $(x_m, t), (m = 0(1)N)$ for any time level, both the knot values and derivatives of the u_N and y_N can be expressed as

$$\begin{aligned} (.)_m &= ()_{m+1} + 4()_m + ()_{m-1} \\ (.)_m^{'} &= \frac{3}{h}((()_{m+1} - ()_{m-1}) \\ (.)_m^{''} &= \frac{6}{h^2}((()_{m+1} - 2()_m + ()_{m-1}). \end{aligned} \tag{4.12}$$

If the nodal values in the equalities (4.12) are substituted in the Eqs.(4.10),(4.11), the following system of equations is acquired

$$\begin{aligned} &\mu_1\delta^{n+1}_{m-3} + \mu_2\delta^{n+1}_{m-2} + \mu_3\delta^{n+1}_{m-1} + \mu_4\delta^{n+1}_m + \mu_5\delta^{n+1}_{m+1} + \mu_6\delta^{n+1}_{m+2} + \mu_7\delta^{n+1}_{m+3} = \\ &\quad \mu_1\delta^n_{m-3} + \mu_2\delta^n_{m-2} + \mu_3\delta^n_{m-1} + \mu_4\delta^n_m + \mu_5\delta^n_{m+1} + \mu_6\delta^n_{m+2} + \mu_7\delta^n_{m+3} \end{aligned} \tag{4.13}$$

$$\begin{aligned} &\rho_1\Psi^{n+1}_{m-3} + \rho_2\Psi^{n+1}_{m-2} + \rho_3\Psi^{n+1}_{m-1} + \rho_4\Psi^{n+1}_m + \rho_5\Psi^{n+1}_{m+1} + \rho_6\Psi^{n+1}_{m+2} + \rho_7\Psi^n_{m+3} = \\ &\quad \rho_1\Psi^n_{m-3} + \rho_2\Psi^n_{m-2} + \rho_3\Psi^n_{m-1} + \rho_4\Psi^n_m + \rho_5\Psi^n_{m+1} + \rho_6\Psi^n_{m+2} + \rho_7\Psi^n_{m+3} \end{aligned} \tag{4.14}$$

in which

$$\mu_1 = \frac{1}{140} - \frac{3\varepsilon}{10h}, \quad \mu_2 = \frac{120}{140} - \frac{72\varepsilon}{10h}, \quad \mu_3 = \frac{1191}{140} - \frac{45\varepsilon}{10h}, \quad \mu_4 = \frac{2416}{140} + \frac{240\varepsilon}{10h},$$

$$\mu_5 = \frac{1191}{140} - \frac{45\varepsilon}{10h}, \quad \mu_6 = \frac{120}{140} - \frac{72\varepsilon}{10h}, \quad \mu_7 = \frac{1}{140} - \frac{3\varepsilon}{10h},$$

and

$$\rho_1 = \frac{1}{140} - \frac{3\varepsilon}{10h} - (\frac{\kappa}{20})\frac{\Delta t}{2}, \qquad \rho_2 = \frac{120}{140} - \frac{72\varepsilon}{10h} - (\frac{56\kappa}{20})\frac{\Delta t}{2},$$

$$\rho_3 = \frac{1191}{140} - \frac{45\varepsilon}{10h} - (\frac{245\kappa}{20})\frac{\Delta t}{2}, \qquad \rho_4 = \frac{2416}{140} + \frac{240\varepsilon}{10h},$$

$$\rho_5 = \frac{1191}{140} - \frac{45\varepsilon}{10h} + (\frac{245\kappa}{20})\frac{\Delta t}{2}, \qquad \rho_6 = \frac{120}{140} - \frac{72\varepsilon}{10h} + (\frac{56\kappa}{20})\frac{\Delta t}{2},$$

$$\rho_7 = \frac{1}{140} - \frac{3\varepsilon}{10h} + (\frac{\kappa}{20})\frac{\Delta t}{2}.$$

Firstly of all, parameter δ^0 must be known to be able to begin the iteration process. Then, this parameter is found from the initial condition and its first derivative in Eq.(1.2). As explained in section 3, firstly, system (4.13) is solved for δ^{n+1}. Later, the founded values are utilized instead of Ψ^n in system (4.14). The parameter δ^1 is computed via the parameter δ^0 obtained using Eq.(4.12). The calculation process can be repeated till the requested time level.

4.1. Stability Analysis

To obtain the stability analysis of (4.13) and (4.14) systems with the cubic B-spline Galerkin finite element method, the Fourier method [32] is used. For stability analysis in the nonlinear term yy_x in Equation (3.4), the local constant Z will be used instead of y. If the Fourier modes given in section 1.3 are substituted in (4.13), (4.14) systems, respectively and also the Euler formula given in section (3.1) is used , it is obtained growth factors presented in the following form

$$\rho_1 = \frac{A_2 - iB_2}{A_2 + iB_2}, \quad \rho_2 = \frac{A_2 - iC_2}{A_2 + iC_2}, \tag{4.15}$$

$$A_2 = \frac{1}{70}c_1 - \frac{3\varepsilon}{5h}c_2, B_2 = 0, C_2 = \frac{z_m \Delta t}{20}c_3$$

$$c_1 = \frac{1}{70}(cos3\Phi + 120cos2\Phi + 1191cos\Phi + 1208), c_2 = -\frac{3\varepsilon}{5h}(cos3\Phi + 24cos2\Phi + 15cos\Phi + 40),$$

$$c_3 = cos3\Phi + cos2\Phi + cos\Phi.$$

It is $|\rho_1| = |\rho_2| = 1$ from Equation (4.15) and therefore $|\rho_1|.|\rho_2| = 1$. It can be clearly stated that systems (4.13) and (4.14) are unconditionally stable. Because, the conditions $|\rho_1| \leq$ and $|\rho_2| \leq 1$ are satisfied.

5. Numerical experiments and comparisons

This section presents a comparison with some of those found in the literature with numerical solutions obtained by implementing suggested two schemes on two examples for the EW equation. To demonstrate the accuracy of both schemes, the error norms L_2, L_∞ and conservation constants I_1, I_2, I_3 given in the following are computed

$$L_2 = ||U - U_N||_2 = \sqrt{h\sum_{j=0}^{N}(U - U_N)^2}$$

$$L_\infty = ||U - U_N||_\infty = \max_j |U - U_N|.$$

and

$$I_1 = \int_{x_L}^{x_R} U(x,t)dx,$$

$$I_2 = \int_{x_L}^{x_R} [U^2(x,t) + \varepsilon U_x^2(x,t)]dx,$$

$$I_3 = \int_{x_L}^{x_R} [U^3(x,t)]dx.$$

Example 5.1. In this example, it has been considered the test problem given with boundary conditions $U \to 0$ as $x \to \infty$, known as single solitary wave and having the analytical solution as follows

$$U = (x,t) = 3csech^2[k(x - x_0 - vt)]$$

in which the width of the solitary wave is $k = 1/\sqrt{4\varepsilon}(\varepsilon = 1)$, the velocity of the wave is $v = c$ and the amplitude of the wave is $3c$. For both schemes mentioned above, the conservative constants I_1, I_2, I_3 and the error norms L_2 and L_∞ are computed. For this, the parameter values $x_0 = 10, c = 0.1$ and $c = 0.03$ are taken on the region $[0, 30]$ on time $t = 80$ in Table 1 and Table 2 for $\Delta t = 0.05, h = 0.03$ and $\Delta t = h = 0.05$, respectively. Conservation features I_1, I_2, I_3 and the error norms L_2 and L_∞ acquired by Lie- Trotter splitting technique using quintic B-spline collocation and cubic B-spline Lumped Galerkin methods are compared with solutions of some previous works in literature. Tables 1-2 show

Table 1: For existing schemes, comparison of invariants and error norms of Example 5.1 for $x_0 = 10, c = 0.1, h = 0.03, \Delta t = 0.05$ on [0,30] with those in Ref.[2,5,7,8,9,13,15, 17].

	t	I_1	I_2	I_3	$L_2 x 10^3$	$L_\infty x 10^3$
Scheme I	0	1.199946	0.288000	0.057600	0.000000	0.000000
	10	1.200014	0.288000	0.057600	0.024439	0.032846
	20	1.200039	0.288000	0.057600	0.033170	0.044931
	40	1.200052	0.288000	0.057600	0.037676	0.051012
	80	1.200039	0.288000	0.057600	0.038827	0.051948
Scheme II	0	1.199946	0.288000	0.777600	0.000000	0.000000
	10	1.200012	0.288001	0.777601	0.023366	0.032291
	20	1.200036	0.288001	0.777603	0.032262	0.044170
	40	1.200048	0.288000	0.777607	0.038488	0.050149
	80	1.200036	0.288000	0.777609	0.045836	0.051068
[2]	0	1.19995	0.2880	0.05760	0.000	0.000
	10	1.20010	0.28804	0.05761	0.048	0.033
	20	1.20015	0.28805	0.05761	0.064	0.046
	40	1.20005	0.28800	0.05760	0.049	0.052
	80	1.19998	0.28798	0.05759	0.056	0.053
[9]	10	1.20001	0.287997	0.0576	0.033297	0.033415
	20	1.20004	0.287997	0.0576	0.056561	0.045709
	40	1.20015	0.287997	0.0576	0.098784	0.051895
	80	1.20004	0.287997	0.0576	0.183785	0.095878
[13]	0	1.2000	0.2880	0.0576	0.000	0.0001
	10	1.1985	0.2873	0.0573	0.900	0.618
	20	1.1981	0.2868	0.0572	1.573	0.927
	40	1.1967	0.2860	0.0570	3.475	2.136
	80	1.1964	0.2858	0.0569	7.444	4.373
[17]	0	1.199945	0.288000	0.057600	0.000000	0.000000
	10	1.200014	0.288000	0.057600	0.026141	0.033416
	20	1.200040	0.288000	0.057600	0.038115	0.045711
	40	1.200052	0.288000	0.057600	0.048432	0.051898
	80	1.200041	0.288000	0.057600	0.054761	0.052850
[5]	80	1.20004	0.2880	0.0576	0.03962	0.05446
[7]	80	1.1910	0.2855	0.05582	3.849	2.646
[8]	80	1.23387	0.29915	0.06097	24.697	16.425
[15]	80	1.20004	0.2880	0.0576	0.03882	0.05151

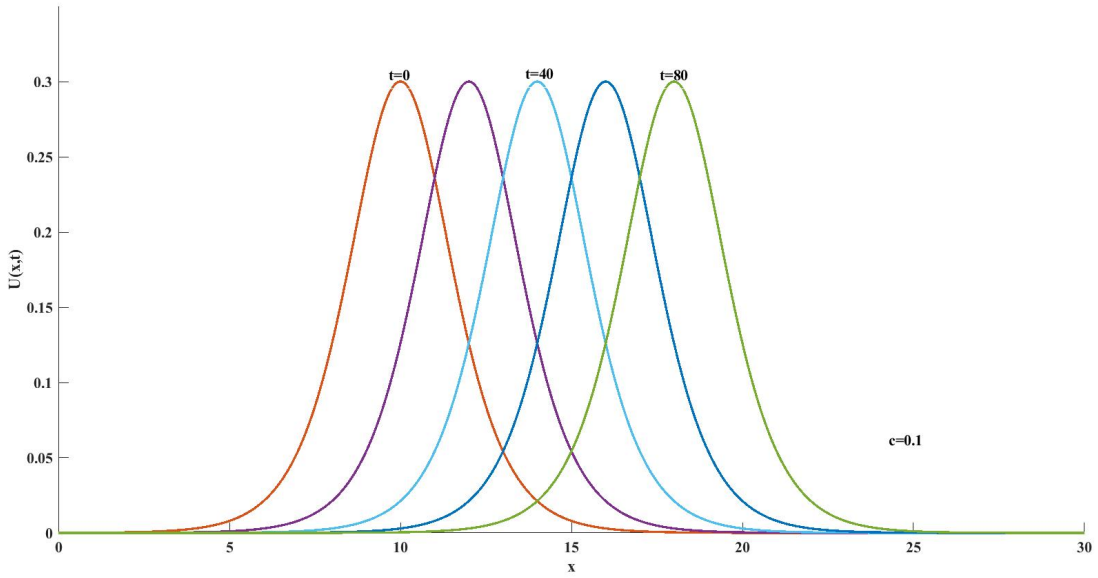

Figure 5.1: The movement of single solitary wave with parameter value $c = 0.1$ for scheme I at t = 0(20)80.

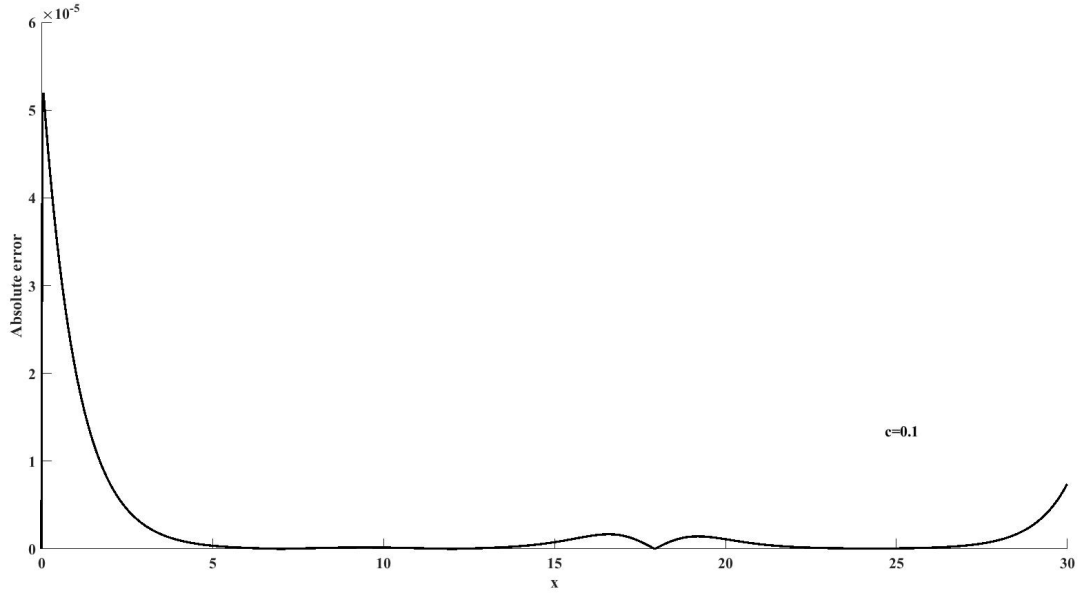

Figure 5.2: Absolute error with parameter value $c = 0.1$ for scheme I at t =80.

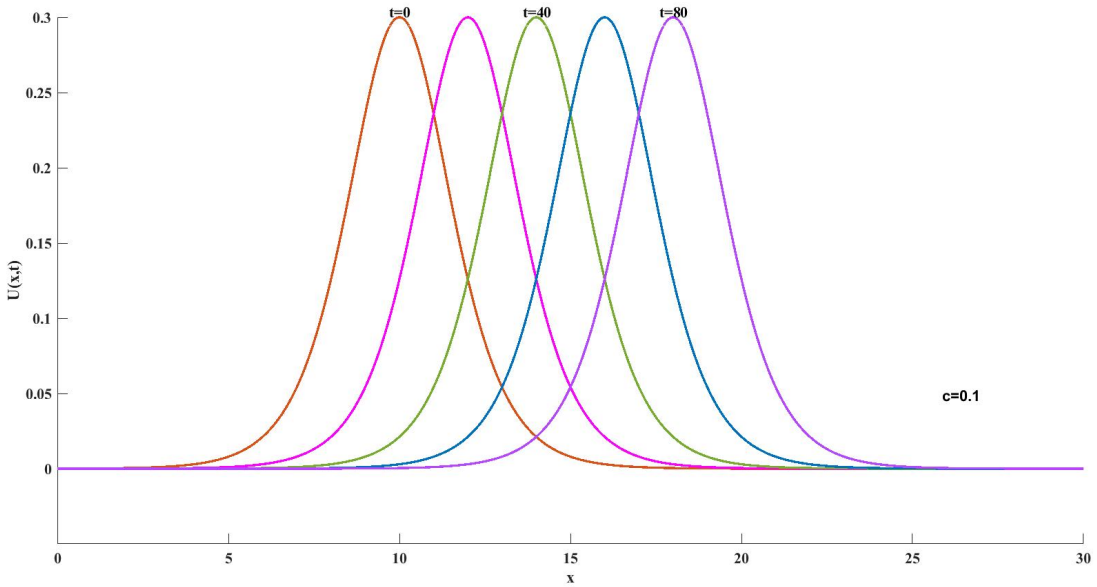

Figure 5.3: The movement of single solitary wave with parameter value $c = 0.1$ for scheme II at t = 0(20)80.

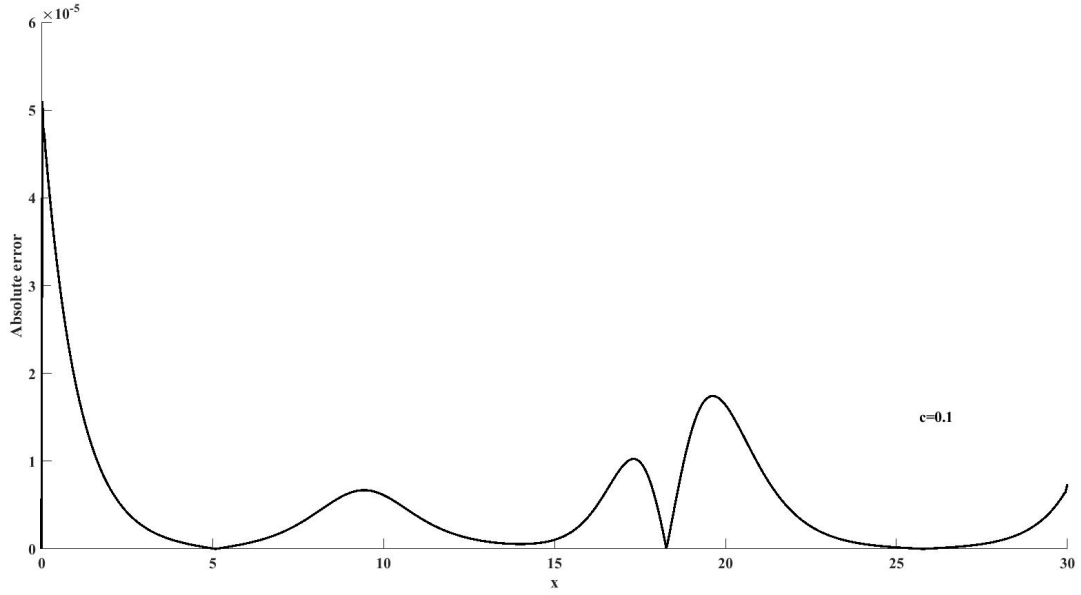

Figure 5.4: Absolute error with parameter value $c = 0.1$ for scheme II at t= 80.

Table 2: For existing schemes, comparison of invariants and error norms of Example 5.1 for $x_0 = 10, c = 0.03, h = \Delta t = 0.05$ on [0,30] with those in Ref.[6,9,10,11,12,17].

	t	I_1	I_2	I_3	$L_2 x10^3$	$L_\infty x10^3$
Scheme I	0	0.359984	0.025920	0.001555	0.000000	0.000000
	10	0.359991	0.025920	0.001555	0.003987	0.012107
	20	0.359998	0.025920	0.001555	0.005516	0.008969
	40	0.360006	0.025920	0.001555	0.008070	0.010555
	80	0.360013	0.025920	0.001555	0.010428	0.013735
Scheme II	0	0.359984	0.025920	0.066355	0.000000	0.000000
	10	0.359991	0.025920	0.066355	0.003982	0.012107
	20	0.359997	0.025920	0.066355	0.005593	0.008969
	40	0.360005	0.025920	0.066355	0.008682	0.010274
	80	0.360012	0.025920	0.066355	0.012944	0.013369
[9]	10	0.359991	0.0259194	0.0015552	0.006478	0.004029
	20	0.359998	0.0259194	0.0015552	0.012628	0.007013
	40	0.360006	0.0259194	0.0015552	0.024398	0.01254
	80	0.360013	0.0259194	0.0015552	0.047152	0.024708
[10]	10	0.35998	0.02592	0.00156	0.008724	0.012107
	20	0.35998	0.02592	0.00156	0.006448	0.008969
	40	0.35999	0.02592	0.00156	0.003515	0.004923
	80	0.36000	0.02592	0.00156	0.001025	0.001483
[11]	10	0.35999	0.02592	0.00156	0.0063	0.0040
	20	0.36000	0.02592	0.00156	0.0123	0.0081
	40	0.36001	0.02592	0.00156	0.0236	0.0165
	80	0.36001	0.02592	0.00156	0.0436	0.0309
[17]	0	0.359984	0.025920	0.001555	0.000000	0.000000
	10	0.359992	0.025920	0.001555	0.003959	0.004029
	20	0.359999	0.025920	0.001555	0.007352	0.007014
	40	0.360007	0.025920	0.001555	0.013007	0.010863
	80	0.360014	0.025920	0.001555	0.021446	0.014528
[6]	80	00.36665	0.02658	0.00162	2.683	1.836
[12]	80	0.36000	0.02592	0.00156	0.013	0.007

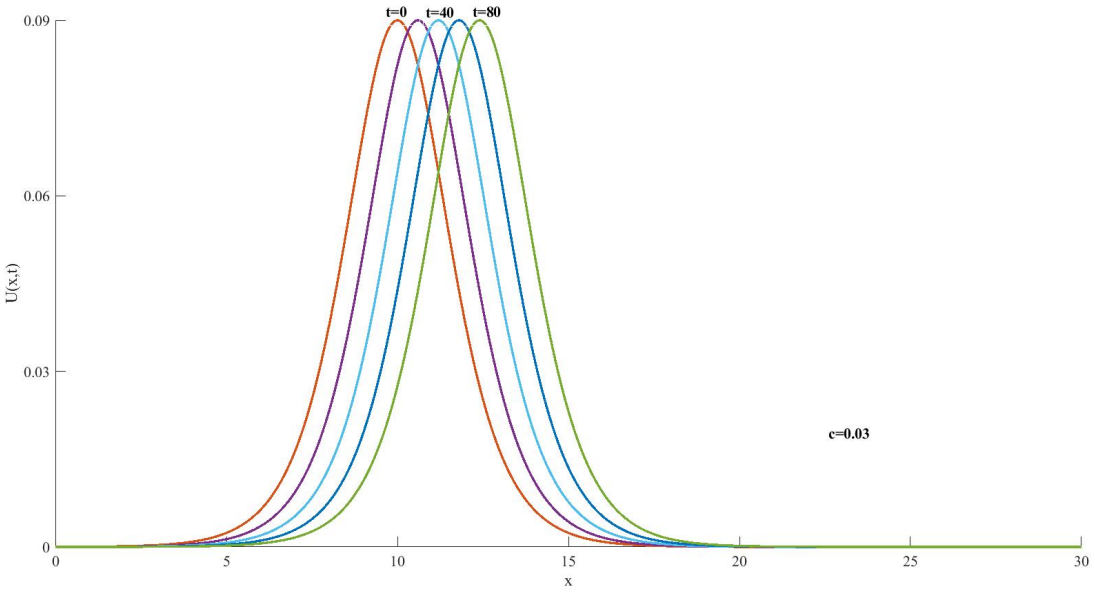

Figure 5.5: The movement of single solitary wave with parameter $c = 0.03$ for scheme I at t = 0(20)80 .

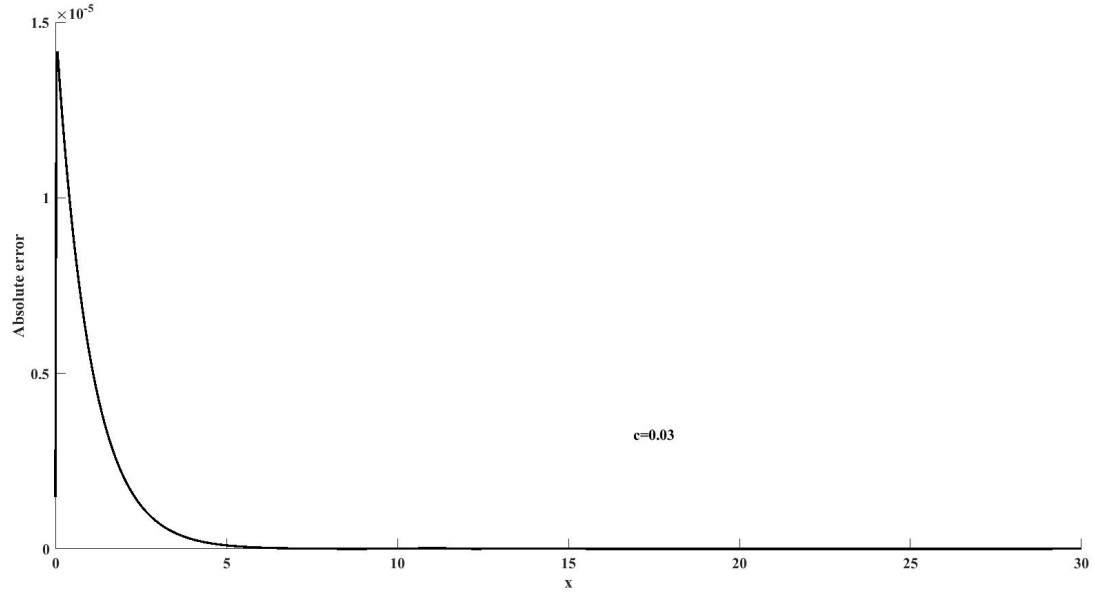

Figure 5.6: Absolute error with parameter value $c = 0.03$ for scheme I at t= 80.

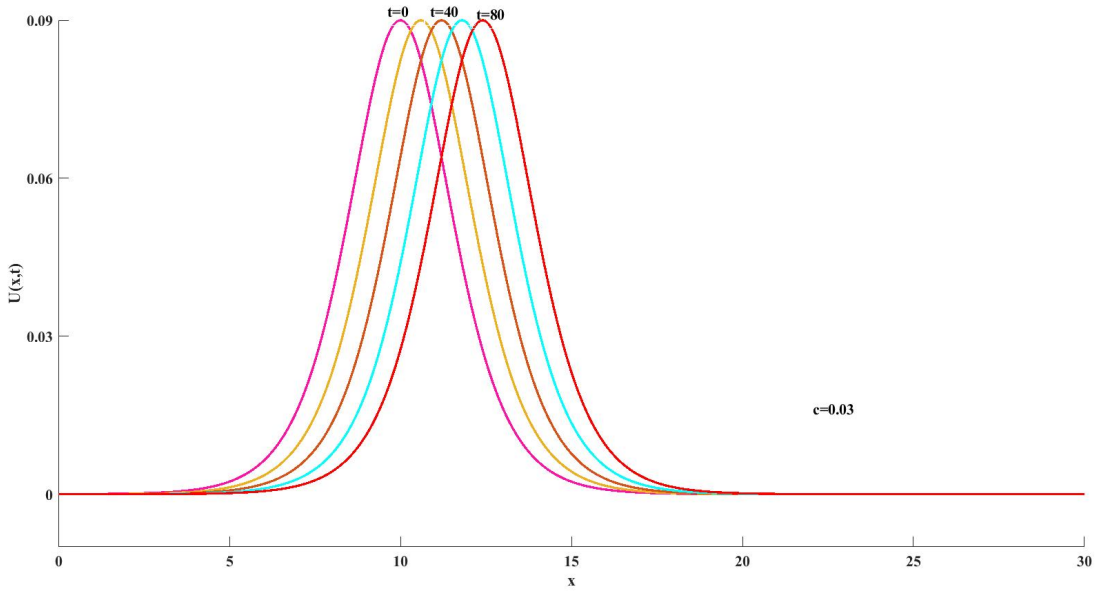

Figure 5.7: The movement of single solitary wave with parameter $c = 0.03$ for scheme II at t = 0(20)80 .

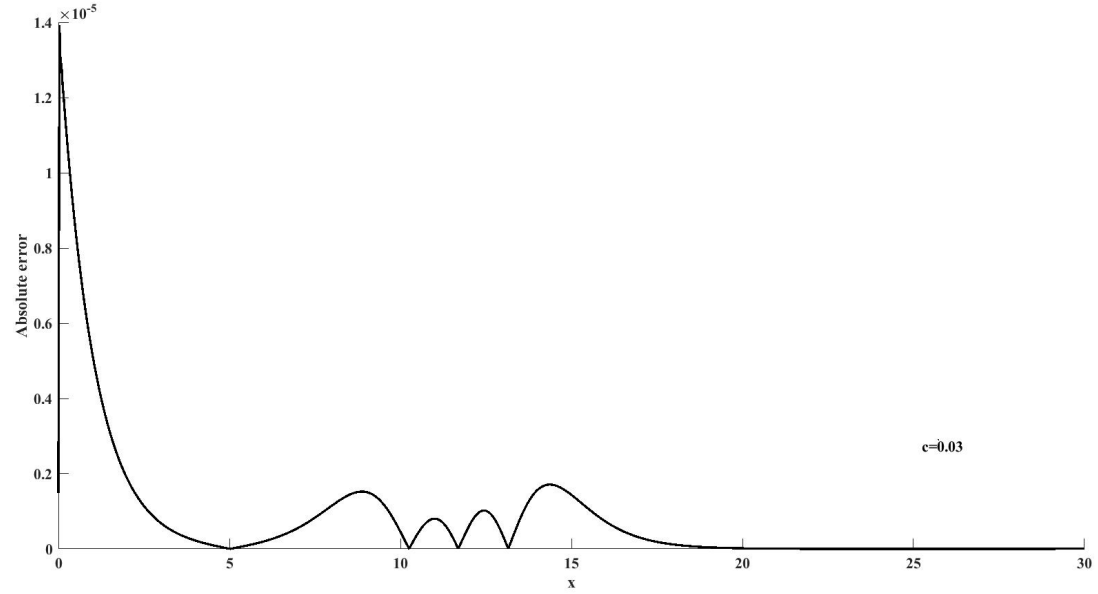

Figure 5.8: Absolute error with parameter value $c = 0.03$ for scheme II at t= 80.

Table 3: A comparison of invariant results of Example 5.2 for $h = 0.05, \Delta t = 0.025$ with those in Ref.[18]

		Scheme I			Scheme II			[18]		
ε	t	I_1	I_2	I_3	I_1	I_2	I_3	I_1	I_2	I_3
0.05	0	1.77245	1.31598	1.02333	1.77245	1.31598	1.02333	1.77245	1.31598	1.02333
	3	1.77250	1.31609	1.02347	1.77245	1.31598	1.02333	1.77245	1.31574	1.02346
	6	1.77250	1.31609	1.02347	1.77245	1.31598	1.02333	1.77245	1.31563	1.02354
	9	1.77250	1.31609	1.02347	1.77245	1.31598	1.02333	1.77245	1.31563	1.02354
	12	1.77250	1.31609	1.02347	1.77245	1.31598	1.02333	1.77245	1.31561	1.02354
0.01	0	1.77245	1.26585	1.02333	1.77245	1.26585	1.02333	1.77245	1.26585	1.02333
	3	1.77251	1.26598	1.02353	1.77245	1.26585	1.02333	1.77245	1.26497	1.02497
	6	1.77251	1.26598	1.02353	1.77245	1.26585	1.02333	1.77245	1.26444	1.02543
	9	1.77251	1.26598	1.02353	1.77245	1.26585	1.02333	1.77245	1.26426	1.02548
	12	1.77251	1.26598	1.02353	1.77245	1.26585	1.02333	1.77245	1.26418	1.02548

that the numerical solutions obtained with both schemes for error norms are lower than ones of the compared approaches. It can be said in the aftermath of the obtained results from both approaches that I_1 is conserved and I_2 and I_3 are more conservative according to the studies given in the Tables 1-2. Figures 1-8 displays movements of single solitary wave and absolute errors for $\Delta t = 0.05, h = 0.03$ and speed values $c = 0.1$ and $c = 0.03$ for both approaches at $t = 0(20)80$ and $t = 80$ respectively. It can be clearly seen from these figures that single solitary wave whose shapes, amplitudes and speeds are quiet conservative during movement to right .

Example 5.2. Our second example concentrates on the solitary waves evolution of the EW equation using the Maxwellian initial condition given in the following form [7]

$$U(x,0) = exp(-(x-20)^2).$$

The invariant values of both approaches have been calculated for different values of $\varepsilon = 0.05, \varepsilon = 0.01$ and parameters $\Delta t = 0.025$, $h = 0.05$ on [0,30] and compared with those in a recent study [18]. It can be clearly stated from Table 3 that the invariant results obtained with approach 2 are more perfect than those of approach 1 and more consistent than those given in Ref.[18].

6. Conclusion

In the present work, approximate solutions of EW equation are acquired Lie- Trotter splitting technique via quintic B-spline Collocation and cubic B-spline Galerkin FEMs. The presented schemes are implemented to two test problem to evaluate the correctness and performance of both methods. The error norms with the conservation properties are computed. It can be seen that the recommended methods present very good solutions. The expository example given in the study demostrate that the error norms are quite small and the conservation properties are almost compatible. Looking at the results of this study, quintic B-spline collocation and cubic B-spline Lumped Galerkin method combined with Lie–Trotter splitting technique applied for approximate solutions of the EW equation are to a good extent numerical approach. Last of all, both methods can be used effectively and appropriately in other nonlinear partial differential equations utilized in many areas.

Acknowledgements

The author would like to express their sincere thanks to the editor and the anonymous reviewers for their helpful comments and suggestions.

Funding

There is no funding for this work.

Availability of data and materials

Not applicable.

Competing interests

There are no competing interests.

Author's contributions

The author contributed to the writing of this paper. The author read and approved the final manuscript.

References

[1] P.J.Morrison, J.D. Meiss, J.R. Carey, Scattering of RLW solitary waves, Physica D., 11 (1981), 324–336.
[2] İ.Dağ, B.Saka, A cubic B-spline collocation method for the EW equation, Math. Comput. Appl., 9(3),2004,381–392.
[3] K. R.Raslan, A computational method for the equal width equation, Int. J. Comput. Math., 81 (1), 2004,63–72.

[4] D. Irk, B. Saka, İ Dağ, Cubic spline collocation method for the equal width equation, Hadronic Journal Supplement, 18 (2003), 201-214.
[5] H.Fazal-i, A. Inayet, A.Shakeel, Septic B-spline Collocation method for numerical solution of the Equal Width Wave (EW) equation, Life Science Journal, 10 (2013), 253-260.
[6] A.Dogan, Application of the Galerkin's method to equal width wave equation, Appl. Math. Comput., 160 (2005), 65–76.
[7] L.R.T.Gardner, G.A.Gardner, Solitary waves of the equal width wave equation, J. Comput. Phys., 101 (1992), 218–223.
[8] S.Güleç, Numerical Solutions of partial differantial equations using Galerkin finite element method, Master Thesis, Nigde University, Turkey, 2007.
[9] M. A. Banaja, H. O. Bakodah Runge-Kutta integration of the equal width wave equation using the method of lines, Math. Probl. Eng., (2015), 1-9.
[10] B.Saka A finite element method for equal width equation, Appl. Math. Comput.,(175) 2006, 730–747.
[11] A.Esen,S. Kutluay, A linearized implicit finite difference method for solving the equal width wave equation, Int. J. Comp. Math., 83 (2006) 319–330.
[12] A.Esen, A numerical solution of the equal width wave equation by a lumped Galerkin method, Appl. Math. Comput., 168 (2005),270–282.
[13] S.I.Zaki, A least-squares finite element scheme for the EW equation, Comput. Meth. Appl. Mech. Eng., 189 (2000), 587–594.
[14] T.Roshan, A Petrov-Galerkin Method for Equal width equation, Applied Mathematics and Computation, 218 (2011), 2730-2739.
[15] A.H.A. Ali, Spectral method for solving the equal width equation based on Chebyshev polynomials, Nonlinear Dyn 51 (2008) 59-70.
[16] L.R.T.Gardner, G.A. Gardner, F.A.Ayoup, N.K. Amein, Simulations of the EW undular bore, Communications in Numerical Methods in Engineering, 13 (1997), 583-592.
[17] İ.Çelikkaya, Operator Splitting Solution of Equal Width Wave Equation Based on the Lie-Trotter and Strang Splitting Methods, Konuralp Journal of Mathematics, 6 (2) (2018) 200-208.
[18] NM.Yağmurlu, AS.Karakaş, Numerical Solutions of the EW Equation By Trigonometric Cubic B-spline Collocation Method Based on Rubin-Graves Type Linearization, Numerical Methods for Partial Differential Equations 36 (5),2020, 1170-1183.
[19] NM.Yağmurlu, AS.Karakaş, A Novel Perspective for Simulations of the MEW Equation By Trigonometric Cubic B-spline Collocation Method Based on Rubin-Graves Type Linearization, Computational Methods for Differential Equations, DOI: 10.22034/CMDE.2021.47358.1981
[20] S.Özer, Numerical solution of the Rosenau–KdV–RLW equation by operator splitting techniques based on B-spline collocation method,Numer Methods Partial Differential Eq., 35 (2019), 1928–1943 (2019),1–16, DOI: 10.1002/num.22387.
[21] Y. Dereli and R. Schaback, The Meshless Kernel-Based Method of Lines for solving the Equal Width Equation, Georg-August G¨ottingen University institut for Numerische and Angewandte Mathematik Preprint-Serie, Number:2010/27.
[22] B. Saka, I. Dağ, Y. Dereli and A. Korkmaz, Three different methods for numerical solutions of the EW equation, Engineering Analysis with Boundary Elements, 32 (2008) 556-566.
[23] S.Özer, Two efficient numerical methods for solving Rosenau-KdV-RLW equation, Kuwait J. Sci., 48 (1),2021, 14-24.
[24] A.Başhan, Y.Uçar¸ NM.Yağmurlu and A. Esen, A new perspective for quintic B-spline based Crank-Nicolson-differential quadrature method algorithm for numerical solutions of the nonlinear Schrödinger equation, Eur. Phys. J. Plus, 133 (12), (2018), https://doi.org/10.1140/epjp/i2018-11843-1.
[25] A.Başhan, NM.Yağmurlu, Y.Uçar¸ and A. Esen, A new perspective for the numerical solution of the Modified Equal Width wave equation, Math Meth Appl Sci. 44 (2021), 8925–8939, DOI: 10.1002/mma.7322.
[26] A.Başhan, An effective approximation to the dispersive soliton solutions of the coupled KdV equation via combination of two efficient methods, Computational and Applied Mathematics, (2020), 39 (80), https://doi.org/10.1007/s40314-020-1109-9.
[27] A. Başhan, A novel approach via mixed Crank–Nicolson scheme and differential quadrature method for numerical solutions of solitons of mKdV equation,Pramana – J. Phys. (2019) 92(84),https://doi.org/10.1007/s12043-019-1751-1
[28] PJ. Olver, Euler operators and conservation laws of the BBM equation, Math. Proc. Camb. Phil. Soc., 85 (1979) ,143-160.
[29] P. M. Prenter, Splines and variational methods, John Wiley, New York, NY, 1975.
[30] H. Holden et al., Splitting methods for partial differential equations with rough solutions, European Mathematical Society, Publishing House, Zürich, 2010.
[31] J.VonNeumann, R. D.Richtmyer, A Method for the Numerical Calculation of Hydrodynamic Shocks, J. Appl. Phys., Vol:21, (1950), 232-237.
[32] G. D. Smith, Numerical solutions of partial differential equations: Finite difference methods, Clarendon Press,Oxford, 1985.
[33] M.Seydaoglu, U. Erdoğan, T.Öziş¸ Numerical solution of Burgers' equation with high order splitting methods, J. Comput. Appl. Math., Vol: 291, (2016) 410–421.
[34] J. Geiser, Iterative Splitting Methods for Differential Equations, CHAPMAN and HALL/CRC., Numerical Analysis and Scientific Computing, Boca Raton, 2011.